

See discussions, stats, and author profiles for this publication at: <https://www.researchgate.net/publication/268561945>

# Classification of airfoils by abnormal behavior of lift curves at low Reynolds number

Conference Paper · June 2006

DOI: 10.2514/6.2006-3179

CITATIONS

14

READS

220

5 authors, including:



[Sutthiphong Srigrarom](#)

National University of Singapore

63 PUBLICATIONS 150 CITATIONS

[SEE PROFILE](#)



[Di Bao Wang](#)

Egis Technology

28 PUBLICATIONS 71 CITATIONS

[SEE PROFILE](#)

Some of the authors of this publication are also working on these related projects:



3D Dynamic UAV Detection and Tracking (MBZIRC project) [View project](#)

# CLASSIFICATION OF AIRFOILS BY ABNORMAL BEHAVIOR OF LIFT CURVES AT LOW REYNOLDS NUMBER

Di-Bao WANG<sup>1</sup>, Chi Seng LEE<sup>2</sup>, Fei-Bin HSIAO<sup>1</sup>, Yen Hock LIM<sup>3</sup>, Sutthiphong SRIGRAROM<sup>3</sup>

1. Institute of Aeronautics and Astronautics, National Cheng Kung University, Tainan, TAIWAN.

2. School of Aerospace Engineering, Universiti Sains Malaysia, Penang, MALAYSIA.

3. School of Mechanical and Production Engineering, Nanyang Technological University, SINGAPORE.

## Abstract

Flow phenomena at low Reynolds number are more complicated than those occurring at high Reynolds number (flow regimes of typical flight). They present unfavorable aerodynamic characteristics and, they are poorly understood. This paper tries to classify airfoils according to the type of pattern showed by its corresponding lift coefficient ( $C_L$ ) curve. Preliminary study of data of over 45 published airfoils reveals that the shape of  $C_L$  curve is strongly related to the combination of maximum thickness ( $t/c$ ), camber, and the shape of the trailing edge. This paper is observation-based, and it is thought that the result obtained may exert some influence on future designs of high performance and improved stability low Reynolds number airfoils, where current designers are still constrained to the "trial and error" method, which usually leads to lengthy and costly design processes.

The aim of this paper is also to determine the reasons for the abnormal behavior of the lift curves for various airfoils by investigating their pressure distribution and flow line plots using a computational fluid dynamics (CFD) program and also find common physical parameters between airfoils that may lead to the display of similar undesired flight characteristics in their lift curves. The CFD program "FEMLAB" was first used to model the performance of the various selected airfoils at their respective  $Re$  number. The next stage involved the analysis of flow patterns, pressure distribution and streamline profiles obtained from the simulation results to explain

the various characteristics observed for the airfoils.

Results indicated that the formation of a long trailing edge separation bubble would induce a drastic drop in the lift coefficient due to the collapse of the suction peak and the formation of a short leading edge separation bubble would lead to a sudden jump in the lift coefficient. It was also observed that increasing the camber and leading edge radius would result in the transition of lift behavior from one trend to another. The trailing edge angle also played a significant role in determining the lift characteristics of an airfoil. It is believed that the above findings may be able to exert some influence on the future design of high performance and improved stability low Reynolds number airfoils.

## 1 Introduction

Since the mid 1950's, an increased interest in developing Micro-Aerial Vehicles (MAV) has been expressed by both civilian and military organizations. This has brought up the need for research of the flow problems faced at  $Re$  of 104~105. The idea of a small flying vehicle that could be used for surveillance was first introduced by Hundley and Gritton in 1992 who thought that it would take just ten years for one to develop a 1 cm wingspan vehicle that would be able to carry a 1g payload. This goal has yet to be achieved. Currently an MAV is defined as having a nominal maximum dimension of 150mm in any direction as required in the MAV research program supported by DARPA. Eventually, the MAVs are required to be capable of flying up to 20 m/s for 30 minutes

while continuously submitting video feed filmed by an onboard camera. This definition places MAVs into the group of birds based on its size and flight speed.

The performance of airfoils at low  $Re$ , incompressible flows are very much different from those that are above  $Re$  of 105 and many undesirable characteristics appear at the low  $Re$  values. The problem lies with the management of the airfoil boundary layer and comprehensive research done in this area will greatly benefit the performance evaluation and stability analysis of MAVs.

Based on the above issues, the purpose of this paper is to:

1. Provide classifications of various airfoils, based on observations of flow behavior at low Reynolds number
2. Obtain Computational Fluid Dynamics (CFD) simulation results for various airfoils.
3. Compare CFD simulation results with experimental results from previous research.
4. Arrive at explanation for performance characteristics of various airfoils.
5. Find common physical parameters and suggest general trends for airfoils displaying the same performance characteristics.

The analysis can be done by: a) Analyze simulation results to verify Laminar Separation Bubble Theory, b) compare  $C_L$  v.s. AoA (Angle of Attack) plots from simulation and experimental results to verify accuracy, and c) study physical parameters of airfoils and suggest general trends that may lead to the generation of a certain undesirable performance characteristics.

## 2 Observation based results

### 2.1 Classification of the airfoils

Airfoils were selected from the series of airfoils found in Ref. 1 and 2. 45 different airfoils are categorized into five groups according to the lift characteristics they exhibit at low Reynolds number ( $60,000 < Re < 300,000$ ). The five groups are :

- i) Recovery (12%): The lift decreases slightly and then recovers as the AoA increases.
- ii) Normal (33%): The lift characteristic is similar to the one at larger Reynolds number.
- iii) Drop (36%): The lift exhibits sudden decrease.
- iv) Jump (7%): The lift exhibits sudden rise.
- v) Jump & drop (12%): The lift characteristic that exhibits both “jump” and “drop” phenomena.

These characteristics are shown in figure 1.

### 2.2 Observation-based results

1 As  $Re$  increases, abnormal behavior tends to fade away. At Reynolds number of more than 300,000, all the peculiar lift characteristics e.g. recovery and drop, tend to become less obvious. The lift curve gradually returns to its normal shape.

2. Combination of  $t/c$  and camber strongly influence the changing of lift curve pattern, as shown in figure 2. Airfoil camber is found to be the governing factor. When airfoils are arranged in order of increasing camber, surprisingly, a trend of gradual shift from recovery to jump and drop is encountered.

3. Low camber and moderate  $t/c$  exhibit good recovery. Study shows that practically all airfoils will indicate the tendency of recovery in their lift characteristic. But different airfoils have different “intensity” of recovery, meaning that some recoveries are very obvious and some are not. It also reveals that camber and thickness of airfoils are primary factors. Low camber (best at 0) and moderate thickness ( $8\% < t/c < 12\%$ ) exhibit good recovery.

4. High  $t/c$ , high camber and a cusp trailing edge initiates jump and drop. Of the 45 airfoils investigated, only five show phenomena of “jump and drop”. All of them present similar geometry characteristics: high thickness ( $11.9\% < t/c < 13.6\%$ ), high camber ( $5.9\% < \text{camber} < 10.2\%$ ), cusp (“downward hook” shape of trailing edge). Among those five airfoils, there exist two different groups, first drop at large AoA, another jump at larger AoA. The location of maximum thickness ( $X_{tmax}$ ) seems to play the

decisive role, as shown in figure 3. The former has more forward  $X_{tmax}$ , whereas the latter  $X_{tmax}$  - is located further aft. Both experience jump (or drop if consider by negatively increasing AoA) at negative AoA.

5. The grater  $t/c$ , the greater the magnitude of “drop”, the increasing thickness of airfoils will increase the decrement of the  $C_L$  value of the drop regime.

6. With deflected flaps,  $C_L$  increases uniformly. Five airfoils are tested with deflected flaps. When compare to the clean airfoil, the  $C_L$  is found to increase slightly with flaps deflected.

### 2.3 Observation-based discussion

1. Flow regime pertaining to  $Re$ . The scope of present paper is restricted to low  $Re$  with respect to aerodynamic aspect. It is important to realize different flow regime and their corresponding features. Carmichael (1981) had done significant surveys of low  $Re$  airfoils. The following discussion from  $1,000 < Re < 200,000$  is a modified version of Carmichael’s original work.

In the range between  $1,000 \leq Re_c \leq 10,000$ , the boundary layer flow is laminar and it is very difficult to cause transition to turbulent flow. The dragon fly and the house fly are among the insects that fly in this regime. The dragon fly wing has a saw tooth single surface airfoil. It has been speculated that eddies in the troughs help keep the flow from separating. The house fly wing has large numbers of fine hair-like elements projecting normal to the surface. It is speculates that these promote eddy-induced energy transfer to prevent separation. Indoor Mica Film type model airplanes also fly in this regime. It has been found that both blunt leading and trailing edges enhance the aerodynamic performance.

For chord Reynolds number between 10,000 and 30,000, the boundary layer is completely laminar and artificial tripping has not been successful. Experience with hand-launched glider models indicates that when the boundary layer separates it does not reattach.

The range  $30,000 \leq Re_c \leq 70,000$  is of great interest to MAV designers as well as

model aircraft builders. The choice of an airfoil section is very important in this regime since relatively thick airfoils (i.e., 6% and above) can have significant hysteresis effects caused by laminar separation with transition to turbulent flow. Also below chord Reynolds numbers of about 50,000, the free shear layer after laminar separation normally does not transition to turbulent flow in time to reattach. Near the upper end of this range, the critical Reynolds number can be decreased by using boundary layer trips. Thin airfoil sections (i.e., less than 6% thick) at the upper end of this regime can exhibit reasonable performance.

At Reynolds number above 70,000 and below 200,000 extensive laminar flow can be obtained and therefore airfoil performance improves although the laminar separation bubble may still present a problem for a particular airfoil. Small radio controlled model airplanes fly in this range.

Above  $Re_c$  of 200,000, airfoil performance improves significantly and there is a great deal of experience available from large soaring birds, large radio controlled model airplanes, human powered airplanes, etc.

2. Separation bubble. The abnormal behavior of lift curve showed previously in this paper is believed to relate very much to the existence of separation bubble. A separation bubble is a region of locally separated flow on the airfoil. It occurs on the upper surface of most airfoil at  $Re < 50,000$ . The extent of this region depends on the operational parameters ( $Re$ , AoA, free stream turbulence) and airfoil geometry ( $t/c$ , camber, surface quality). The complicated combination among above quantities determines the characteristic of the separation bubble formed.

Since in the 1960s, numerous papers about the discussion of separation bubble have been published. Among them are: Tani (1964), Horton (1967), J.F.Marchman (1986), Shun and Marsden (1993), Lin and Pauley (1993), etc. However, practically all of them share the similar fundamental about the formation of a separation bubble. The model proposed by Tani and Horton is considered as the most detail one

and following discussion is based on the essence of their paper.

Basically, the formation of separation bubble occurs within 3 stages (see figure 4). 1) Laminar separation (S). When a laminar boundary layer encounters an adverse pressure gradient, it generates sufficient strength and separates from the airfoil. This is point S in figure 4. 2) Transition (T). The separation leads to the formation of the shear layer over the bubble. The shear layer becomes very unstable and shows characteristic flow reversal near the surface. At point T, the shear layer makes a transition to turbulent flow. Before transition, the reversal flow is very slow, and this area is sometimes referred to as dead-air region. The static pressure in the bubble seen to be fairly constant over the bubble until transition. 3) Reattachment (R). After transition, the magnitude of the reverse flow increases and vortex type flow is seen in the bubble. There is an abrupt rise in pressure near the reattachment point. As the turbulent shear layer entrains high-energy external flow, pressure recovery becomes possible, and the bubble reattaches at point R.

According to the classification made by Ward and Tani, there are 2 type of bubble, distinguished by their effect on the flow field around airfoil. 1) Short bubble. One that affects only the local pressure distribution, therefore little effect on the airfoil performance. 2) Long bubble. One that can alter macroscopically the airfoil pressure distribution, further causes the collapse of the suction peak (see figure 5).

A short bubble usually developed just behind the leading edge, while a long bubble starts far behind the leading edge (see figures 6 and 7). It is speculated that a separation bubble may contracts or elongates as AoA increases, depending on the complicated combination of operational parameters and airfoil geometry as mentioned earlier. Unfortunately, up to present, the authors haven't been able to reveal the answer which can help to explain several flow problems regarding low  $Re$  aerodynamics and unusual lift curve pattern that follows. Further and more detail study and investigation of this phenomenon is recommended for they may

induced the development of UAV, MAV, or any vehicles designed to operate in the low  $Re$  regime.

### 3 CFD simulation procedures and results

#### 3.1 Method of Investigation

In parallel to the observation, Computational Fluid Dynamics (CFD) simulations are used for comparative purpose. AutoCAD will first be used to generate the 2D profile of the 8 chosen airfoils. The airfoil profile will then be imported into the CFD software "FEMLAB" which will be used to generate the required simulation results. The range of  $Re$  number will be from 40,000~100,000 which is well within the definition of Low  $Re$ . Individual plots of each airfoil at AoA ranging from  $-6^\circ$  to  $20^\circ$  will be obtained and their corresponding  $C_L$  V.S. AoA plots will be plotted with the use of Excel and Matlab for comparison with the experimental plots obtained from previous research as in Ref. 1 and 2. The physical parameters of each of the 8 airfoils will also be studied to come up with the general trends that may lead to the display of a certain undesirable performance characteristic.

#### 3.2 Selection of Airfoils

Selection criterion was based on the phenomenon of the airfoils performance observed from each group and the airfoils within each group had to have the same Reynolds numbers where the phenomenon was observed, they also had to belong to the same type of application for the airfoil (i.e. they had to be used for aircraft and not sailplanes or turbine and rotor blades). In addition, Reynolds number had to match closely for airfoils between each group also so as to facilitate comparison of the physical parameters of the airfoils within and between the groups.

Out of a total of 91 different airfoils that can be found in Ref. 1 and 2, 8 airfoils have been selected based on the selection criteria listed above. Their classification type,



aerodynamic lift behavior, Reynolds number and general shape profile is listed in Table 1, the respective airfoil technical specification is also listed in Table 2.

As can be observed from Table 1, airfoils displaying similar phenomenon had the same aircraft application and also displayed the same phenomenon at the same Reynolds number. The Reynolds number was chosen to be relatively close to each other so as to facilitate inter-group comparisons for their simulation results and also their physical parameters. The comparisons between the groups will be carried out at  $Re$  of 40k, 60k and 100k. At least 2 airfoils were selected for each group phenomenon for the purpose of comparison within the groups itself, the only exception is for the recover phenomenon, reason being is that no other models of airfoils was found in the two volumes of airfoil data for aircraft application as the rest of the airfoils displaying the recover phenomenon were used for rotor and turbine blades thus rendering them inapplicable to this paper.

### 3.3 Simulation Results

The simulation results from FEMLAB are illustrated in Figure 8~21. Although the range of AoA for each airfoil in this paper is defined as -6 degrees to 20 degrees at 2 degrees interval, only the plots showing the speculated causes for the phenomenon displayed will be included, these figures will be essential in the discussion section later. The plots will have pressure as the surface expression and the contour and flow line expressions are also included to be used in the discussion section.

### 3.4 Discussion of $C_L$ v.s. AoA Plots

From the comparison done in Graphs 1 and 2, it is observed that the general trend in the plots that were charted out from FEMLAB corresponds very much to the plot obtained from experimental results in the wind tunnel experiments done in Ref. 1 and 2.

For example, the FX74-CL5-140MOD displays clearly the “drop and jump”

phenomenon and it happens at around the same AoA as observed in the wind tunnel. Similarly, the MA409 displays the “recover” phenomenon at around the same AoA as observed in the wind tunnel also. These two airfoils were chosen to verify the accuracy of FEMLAB because their plots will have covered all four phenomenon to be discussed in the scope of this paper, namely, “jump”, “drop”, “drop and jump” and “recover”. Therefore, the general trends observed in the airfoil plots using FEMLAB are still valid. Also, it is safe to assume that the general flow patterns around the different airfoils at their varying AoAs are accurate enough for the purpose of analysis.

#### 3.4.1 NACA 2414 at $Re = 60k, 100k$

With reference to Graph 3, the NACA 2414 at  $Re = 60k$  displays a “drop” phenomenon. From Figure 8, at the AoA of  $12^\circ$ , nothing out of the ordinary is observed in the flow patterns. The pressure distribution looks to be alright as the majority of the top surface of the airfoil is covered in blue meaning suction and that is how the lift force on the airfoil is obtained.

In Figure 9 with AoA at  $14^\circ$ , it is observed that a long trailing edge separation bubble has begun to form. This value of AoA corresponds to a drastic drop in the  $C_L$  value as can be seen from the plot in Graph 3. Thus, it is speculated that the formation of a separation bubble at the trailing edge of an airfoil may have altered the airfoil pressure distribution and caused the collapse of the suction peak thus leading to the “drop” phenomenon. The speculation corresponds with the FEMLAB simulation results obtained for the NACA 2414 at  $Re = 100k$ . A long trailing edge separation bubble also starts to form at AoA of  $14^\circ$  which is the onset of the “drop” phenomenon as can be seen in Graph 4.

#### 3.4.2 NACA 2415 at $Re = 60k, 100k$

With reference to Graphs 5 and 6, the NACA 2415 at  $Re = 60k, 100k$  both displays the “drop” phenomenon similar to the NACA 2414. From Figure 10, at an AoA of  $12^\circ$ , a long trailing edge separation bubble is again observed to be formed and this coincides with

the onset of the drop phenomenon as can be seen in Graph 5. This further strengthens our speculation that a long separation bubble at the trailing edge leads to the “drop” phenomenon by causing a collapse of the suction peak.

From Figure 11 at an AoA of  $18^\circ$  for  $Re = 100k$ , it can be seen that the trailing edge separation bubble has disappeared and this is again speculated to result in the  $C_L$  value climbing again as can be observed in Graph 6. The “bursting” of the trailing edge separation bubble has allowed the lift coefficient to pick up again.

#### 3.4.3 MB253515 at $Re = 60k$

With reference to Graph 7, the MB253515 undergoes the “jump” phenomenon. As observed in Figure 12, at an AoA of  $12^\circ$ , it can be seen that there is a break in the flow lines above the leading edge of the airfoil. The leading edge is also the area with the highest pressure distribution as can be seen from the dark color. It is speculated that the strong adverse pressure gradient at the leading edge of the airfoil may have caused a separation in the boundary layer resulting in the breaking up of the flow lines thus inducing the formation of a separation bubble. If this is so, a short leading edge separation bubble would have been formed and this would result in the sudden increase in the lift coefficient as theorized by Mueller and Batill (Ref. 18). The formation of this short leading edge separation bubble at  $12^\circ$  also coincides with the onset of the “jump” phenomenon as can be seen from Graph 7. At AoA of  $16^\circ \sim 20^\circ$ , the short leading edge separation bubble grows and shrinks in size and this accounts for the fluctuations in the  $C_L$  values in that range of AoA.

#### 3.4.4 NACA 6409 at $Re = 60k$

With reference to Graph 8, the NACA 6409 experiences the “jump” phenomenon and the onset of this occurs at around an AoA of  $8^\circ$ . From Figure 13, at an AoA of  $8^\circ$ , it can be seen that for the same reasons as elaborated for the MB253515 above, a short leading edge separation bubble is speculated to be formed due to the adverse pressure gradient. Figure 13 offers a much clearer view of the breaking up of

the boundary layer at the leading edge and also the small region of extremely high pressure distribution as compared to the surroundings. Prior to this AoA of  $8^\circ$ , no boundary layer separation is observed in the simulation results. This further confirms that there is the presence of a short leading edge separation bubble although it is not displayed in the simulation results as the “jump” phenomenon is again observed. Figure 14 also displays the wing for the purpose of illustrating that since there is no formation of the long trailing edge separation bubble, the NACA 6409 at  $Re = 60k$  does not undergo the “drop” phenomenon which is in line with our speculations made so far.

#### 3.4.5 CH10-48-13 at $Re = 100k$

Referring to Graph 9, the CH10-48-13 displays a “drop and jump” phenomenon. From Figure 15, at an AoA of  $4^\circ$ , a long trailing edge separation bubble starts to form and this coincides with the airfoil experiencing the “drop” phenomenon at a range of AoA from  $4^\circ \sim 6^\circ$ . In addition, it can be seen from Figure 16 that at an AoA of  $12^\circ$ , the short leading edge separation bubble is formed and this leads to the onset of the “jump” phenomenon as can be seen in Graph 9. Although the long trailing edge separation bubble is still present in Figure 16, it can be seen that it has actually shrunk in size and circulation as compared to the long trailing edge separation bubble in Figure 15, thus possibly allowing the “jump” phenomenon to take place at the AoA of  $12^\circ$ .

#### 3.4.6 FX74-CL5-140MOD at $Re = 100k$

Referring to Graph 1, the FX74-CL5-140MOD undergoes the “drop and jump” phenomenon similar to the CH10-48-13 airfoil. The observations derived from the FEMLAB simulation results are also very similar to the CH10-48-13. From Figure 17, at an AoA of  $6^\circ$ , a long trailing edge separation bubble starts to form which is slightly off from the “drop” phenomenon observed from Graph 1 at the range of AoA from  $2^\circ \sim 4^\circ$ . In addition, it can be seen from Figure 18 that the “jump” behavior is possibly due to the formation of the short leading edge separation bubble at  $16^\circ$ . The existence of the short leading edge and long

trailing edge separation bubble at the same time complicates matters, thus there must be a compromise between the formation of the two bubbles to allow the “jump” phenomenon to take place.

#### 3.4.7 MA 409 at $Re = 40k$

With reference to Graph 2, the MA 409 airfoil displays the “recover” phenomenon. Not much observations can be derived out of the FEMLAB simulation for this airfoil as no significant leading edge or trailing edge separation bubbles are observed to be formed throughout the entire range of AoA for this paper ( $-6^\circ \sim 20^\circ$ ) thus accounting for the absence of the “drop” and “jump” zones. Figure 19 is attached as an illustration of the simulation results obtained from FEMLAB for this airfoil.

#### 3.4.8 NACA 633018 at $Re = 40k$

This airfoil was done initially to compare with experimental results done at National Cheng Kung University (NCKU), Taiwan. It displays the “jump and drop” phenomenon. From Figure 20, the formation of the short leading edge separation bubble at an AoA of  $12^\circ$  leads to the “jump” behavior and from Figure 21, the formation of the long trailing edge separation bubble at an AoA of  $15^\circ$  lead to the “drop” phenomenon. These results tie in with the experimental results obtained from the wind tunnel experiments done in NCKU, Taiwan.

### 3.5 Summary of Physical Parameters for Individual Airfoils

Comparison of the physical parameters of each airfoil within and between the groups showing the four different flight characteristics at low Reynolds number is taken from the data listed in Table 2 earlier.

### 3.6 Discussion of Relation of Physical Parameters to Airfoil Phenomenon

From Table 2, it is observed that when the airfoils are arranged in an ascending order with respect to their camber, a trend of a gradual shift from “recover” to “drop” to “jump” to

“drop and jump” is observed. This is illustrated in Table 3.

Figure 2 shows the various combinations of  $t/c$  and camber for different airfoils. Although the boundary of each group is not very clear and separate, it is still possible to identify and distinguish certain areas of the plots where the airfoils displaying the various flight characteristics lie. This will help give a general idea of what combinations of thickness and camber will result in what type of flight characteristics.  $C_{Lmax}$  is also observed to increase gradually as the camber increases.

Further comparisons carried out on the airfoils displaying the “drop” v.s. “jump” phenomenon show that those undergoing the “drop” characteristics have a leading edge radius of 2-3 times that of airfoils displaying the “jump” characteristics. It is also observed that airfoils with the “drop and jump” characteristics have leading edge radius values that are in between that of the “drop” characteristic airfoils and the “jump” characteristic airfoils. Thus, increasing the leading edge radius of an airfoil will result in a gradual shift of lift curve behavior from “jump” to “drop and jump” to “drop” characteristic.

It is known that almost all airfoils have the tendency to display a certain amount of the “recover” phenomenon in their lift characteristics, it is just that some have more obvious recovery patterns than the rest. It is observed that a low camber and moderate thickness will have good recovery characteristics as in the case of the MA 409 airfoil.

In addition, further analysis showed that relatively thick airfoils with a high camber and a trailing edge angle of more than  $20^\circ$  or airfoils that possess a cusp trailing edge tends to the “drop and jump” phenomenon. Whether a “drop” or “jump” will be experienced at the high AoA depends on the location of the maximum thickness ( $t/c$ ). The more aft the maximum thickness is located from the leading edge, the higher the probability that an airfoil will experience the “drop” at a low AoA and the “jump” at the high AoA. The same can be said of the reverse situation where the maximum



thickness is located in the more forward position of the airfoil's leading edge. By comparing the physical parameters of the NACA 633018, FX74-CL5-140MOD and CH10-48-13, it can also be said that the “drop and jump” phenomenon can be distinguished from the “jump and drop” phenomenon by the difference in value of the trailing edge angle. Airfoils with a trailing edge angle above  $20^\circ$  will undergo the “drop and jump” phenomenon.

#### 4 Conclusion

The simulations and analysis for the classification of airfoils by abnormal behavior of lift curves at low Reynolds number has been successfully carried out and seemed to be in consistent to the observations discussed at the beginning.

It was observed that the formation of a long trailing edge separation bubble would lead to the “drop” phenomenon and the formation of a short leading edge separation bubble would lead to the “jump phenomenon”. The observations and deductions made were very consistent with all the simulation results of the 8 individual airfoils and their corresponding  $C_L$  v.s. AoA plots. At the angles where there was a “drop” region on the  $C_L$  v.s. AoA plots, the corresponding simulation result would show the onset of the formation of a long trailing edge separation bubble and at angles where there was a “jump” on the  $C_L$  v.s. AoA plots, it was deduced from observation of the pressure and flow profiles that a short leading edge separation bubble was formed. The formation of a trailing edge separation bubble was very obvious from the plots as a re-circulating region was observed, whereas the formation of the leading edge separation bubble was speculated to be formed based on the strong adverse pressure gradient observed at the leading edge and also the separation of the boundary layer observed by the breaking up of the flow lines in the FEMLAB plot.

By carrying out comparisons of the important physical attributes of each airfoil such as the maximum thickness, camber, leading

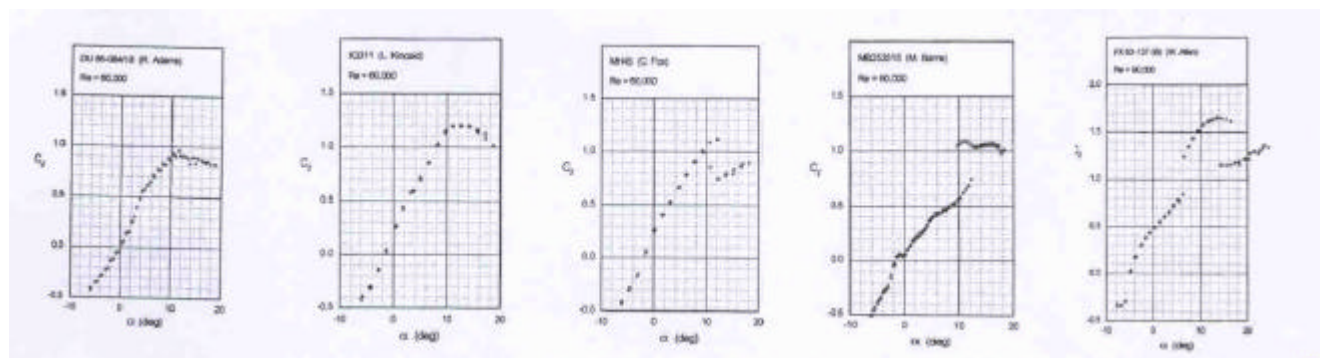
edge radius and the trailing edge angle, it was observed that as camber is increased, the behavior of airfoils shift gradually from “recover” to “drop” to “jump” to “drop and jump”. Camber is the main deciding parameter for this trend, but when the combination of camber and  $t/c$  is identical,  $X_{tmax}$  becomes the deciding factor. It was also observed that increasing the leading edge radius of an airfoil will result in the shift of the behavior of the lift curve from “jump” to “drop and jump” to “drop”. Furthermore, airfoils with low camber and moderate chord thickness shows better recovery patterns in the lift curve. Finally, it was also observed that relatively thick airfoils with a high camber and a trailing edge angle of more than  $20^\circ$  and also airfoils that possess a cusp trailing edge tends towards the “drop and jump” phenomenon. Whether a “drop” or “jump” will be experienced at the high AoA depends on the location of the maximum thickness ( $t/c$ ) and also the trailing edge angle.

Current designers of airfoils for low Reynolds number performance are still constrained to the “trial and error” method due to the limited understanding of airfoil performance at low Reynolds number, thus usually leading to lengthy and costly design processes. The results and observations that were obtained in this paper may offer us some additional insight into the design of airfoils for low Reynolds number performance.

#### References

1. “Summary of Low-Speed Airfoils Data”, volume1, published by SoarTech Publications.
2. “Summary of Low-Speed Airfoils Data”, volume2, published by SoarTech Publications.
3. Thomas J. Mueller, “Aerodynamic Measurements at Low Reynolds Numbers for Fixed Wing Micro-Air Vehicles”, R, Hessert Center for Aerospace Research, University of Notre Dame, September 1999
4. Tani, “Low Speed Flows Involving Bubble Separations”, Progress in Aeronautical Science, Pergamon, New York, pp. 70-103, 1964.
5. Roberts, W. B., “Calculation of Laminar Separation bubbles and their Effect on Airfoil Performance,” AIAA Journal, Vol. 18, No. 1, pp. 25-31, 1980.

6. Horton, H. P., "Laminar Separation Bubbles in two- and three- dimensional Incompressible Flow," Ph.D. Thesis, Univ. of London, Queen Mary College, London, 1968.
7. Ward, J. W., "The Behavior and Effects of Laminar Separation Bubbles on Aerofoils in Incompressible Flow," Journal of the Royal Aeronautical Society, Vol. 67, No. 636, pp. 783-790, 1963.
8. Y.K. Shum and D. J. Marsden, "Separation bubble Model for Low Reynolds Number airfoil Applications" Journal of Aircraft, Vol. 31, No. 4, pp. 761, 1994.
9. M. B. Bragg and A. Khodadoust, "Measurements in a Leading-Edge Separation Bubble due to a Simulated Airfoil Ice Accretion", Journal of Aircraft, Vol. 30, No. 6, pp. 1462, 1991.
10. J. F. Marchman, "Aerodynamic Testing at Low Reynolds" Journal of Aircraft, Vol. 24, No. 2, pp. 107, 1987.
11. Carmichael, B. H. "Low Reynolds number Airfoil Survey." Volume 1, NASA Contractor Report 165803, November 1981.
12. McMasters, J.H and Henderson, M.L., "Low Speed Single Element Airfoil Synthesis", Tech. Soaring, Vol. 2, pg. 1-21, 1980.
13. Hsiao, F.B., Chang, C.Y., Hsu, C.C. and Wang, D.B., "Experimental Study of Aerodynamic Performance for Finite Wing at Low Reynolds Numbers", J. Chinese Society of Mechanical Engineers, Vol. 23, No. 6, pg 517-524, 2002.
14. Pauley, Laura L., Parviz Moin and William C. Reynolds, "The Structure of 2-D Separation", J. Fluid Mech., Vol. 220, pg 397-411, 1990.
15. Ripley, Matthew D. and Laura L. Pauley, "The Unsteady Structure of a 2-D Steady Laminar Separation", Phys. Fluids A, Vol. 5, pg. 3099-3106, 1993.
16. Muti Lin, J.C. and Laura L. Pauley, "Low Reynolds Number Separation on an Airfoil", AIAA Journal, Vol. 34, pg. 1570-1577, 1996.
17. Tatineni, M. and X., Zhong, "Numerical Simulations of Unsteady Low-Reynolds Number Separated Flow Over Airfoils", AIAA 97-1929, July 1997.
18. Mueller, T.J and Batill, S.M., "Experimental Studies of Separation of a Two-Dimensional Airfoil at Low Reynolds Number.", AIAA 80-1440R, Vol. 20, April 1982.
19. Abbott, I.H and Von Doenhoff, A.E, "Theory of Wing Sections Including a Summary of Airfoil Data", New York, Dover Publications, 1959.
20. Laitone, E.V., "Aerodynamic Lift at Reynolds Numbers Below  $7 \times 10^4$ ", AIAA Journal, Vol. 34, No. 9, September 1996.
21. Mueller, T.J. and Delaurier, J.D., "An Overview of Micro Aerial Vehicle Aerodynamics", Fixed and Flapping Wing Aerodynamics for Micro Aerial Vehicle Applications, Reston, VA, AIAA, Inc., 2001
22. O' Meara, M.M. and Mueller, T.J., "Laminar Separation Bubble Characteristics on an Airfoil at Low Reynolds Numbers", AIAA Journal, Vol. 25, No.8, Aug 1987.
23. Pelletier, Alain and Mueller, T.J., "Low Reynolds Number Aerodynamics of Low-aspect-ratio, Thin/Flat/Cambered-plate Wings", Journal of Aircraft, Vol.37, No.5, Sept-Oct 2000, Pg. 825-832.
24. Selig, M.S. et al., "Summary of Low-Speed Airfoil Data Volume 1 & 2", SoarTech Publications, 1995.
25. Schmidt, G.S. and Mueller, T.J., "Analysis of Low Reynolds Number Separation Bubbles Using Semi-empirical Methods", AIAA Journal, Vol. 27, Aug 1989.
26. Mueller, T.J., "The Influence of Laminar Separation and Transition on Low Reynolds Number Airfoil Hysteresis", AIAA, Vol. 22, No.9, Sept 1985.



(a) Recovery (b) Normal (c) Drop (d) Jump (e) Jump and drop  
Figure 1: Lift Characteristics

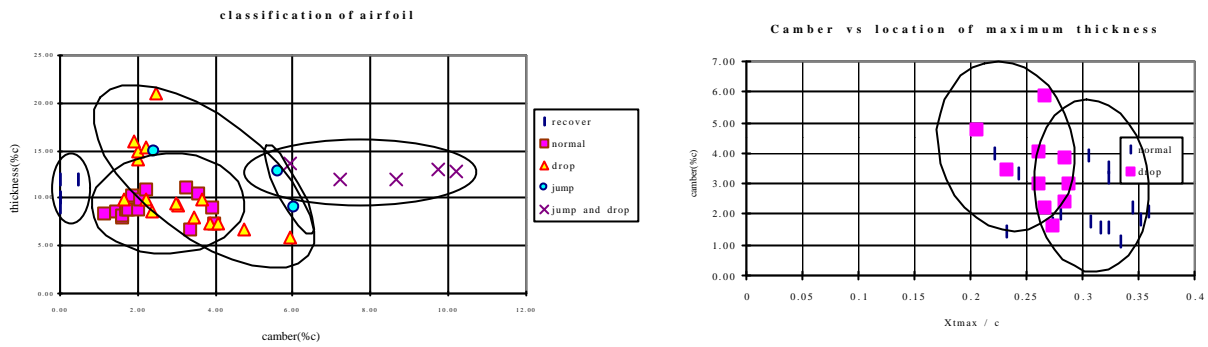


Figure 2 (left) and 3 (right): Characteristics of airfoil and Camber v.s. location of maximum thickness

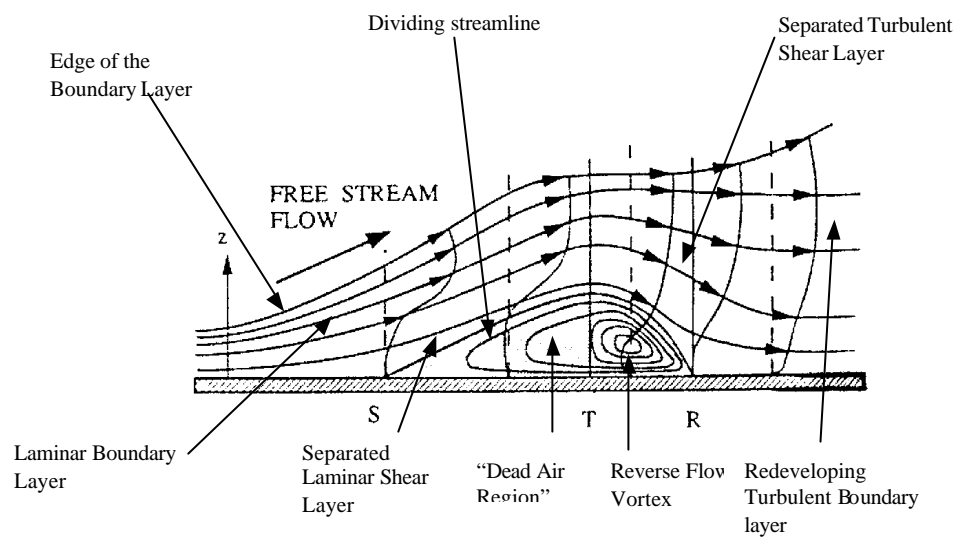


Figure 4: separation bubble

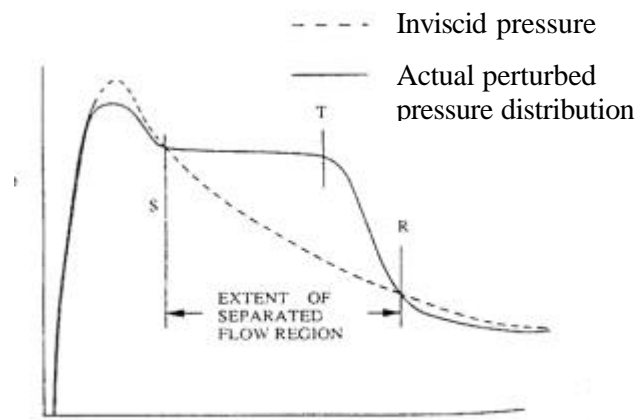


Figure 5:  $C_p$  distribution on upper surface of airfoil

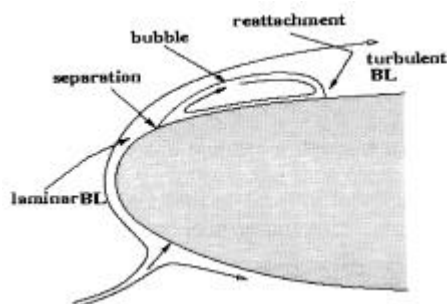


Figure 6: Short bubble

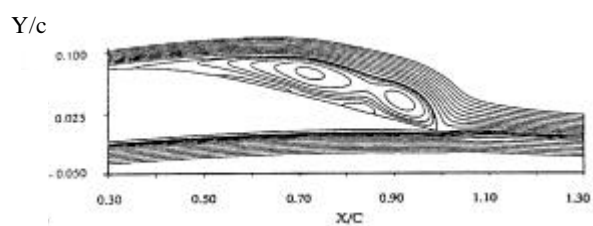


Figure 7 : Long bubble

# CLASSIFICATION OF AIRFOILS BY ABNORMAL BEHAVIOR OF LIFT CURVES AT LOW REYNOLDS NUMBER








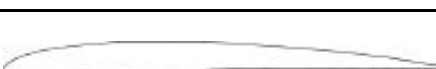
| Name            | Type                   | Profile   | Phenomenon    | Re        |
|-----------------|------------------------|---|---------------|-----------|
| NACA 2414       | Sports Plane           |    | Drop          | 60k, 100k |
| NACA 2415       | Sports Plane           |    | Drop          | 60k, 100k |
| MB253515        | Free Flight Model      |    | Jump          | 60k       |
| NACA 6409       | Free Flight Model      |    | Jump          | 60k       |
| CH10-48-13      | Heavy Lift Cargo Plane |    | Drop and Jump | 100k      |
| FX74-CL5-140MOD | Heavy Lift Cargo Plane |   | Drop and Jump | 100k      |
| NACA 633018     | Free Flight Model      |  | Drop and Jump | 40k       |
| MA 409          | Free Flight Model      |  | Recover       | 40k       |

Table 1: List of Selected Airfoils

| Name            | Thickness/m | Camber/m | Leading Edge Radius/m | Trailing Edge Angle/ degree |
|-----------------|-------------|----------|-----------------------|-----------------------------|
| NACA 2414       | 0.1401      | 0.0188   | 0.0208                | 18.8564                     |
| NACA 2415       | 0.1501      | 0.0186   | 0.0240                | 20.3576                     |
| MB253515        | 0.1496      | 0.0241   | 0.0078                | 18.2663                     |
| NACA 6409       | 0.0903      | 0.0586   | 0.0096                | 12.3303                     |
| CH10-48-13      | 0.1284      | 0.1019   | 0.0138                | 23.6817                     |
| FX74-CL5-140MOD | 0.1308      | 0.0973   | 0.0118                | 22.4039                     |
| NACA 633018     | 0.1200      | 0.1400   | 0.0500                | 5.0000                      |
| MA 409          | 0.0680      | 0.0031   | 0.0028                | 9.9582                      |

Table 2: Airfoil Technical Specification

| Name            | Camber/m | Phenomenon    |
|-----------------|----------|---------------|
| MA 409          | 0.0031   | Recover       |
| NACA 2415       | 0.0186   | Drop          |
| NACA 2414       | 0.0188   | Drop          |
| MB253515        | 0.0241   | Jump          |
| NACA 6409       | 0.0586   | Jump          |
| FX74-CL5-140MOD | 0.0973   | Drop and Jump |
| CH10-48-13      | 0.1019   | Drop and Jump |
| NACA 633018     | 0.1400   | Jump and Drop |

Table 3: Classification of Airfoils According to Camber



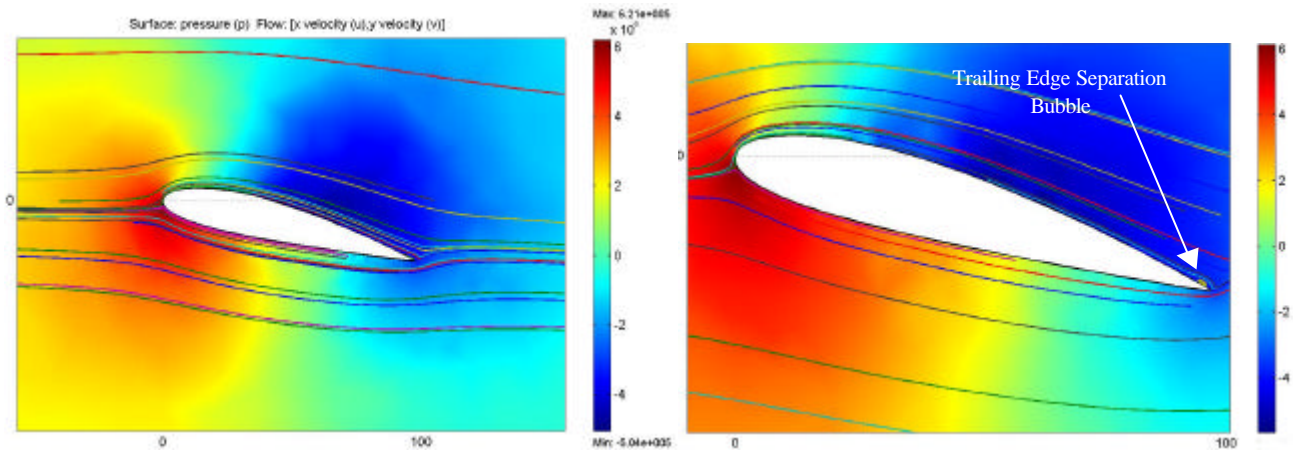


Figure 8 (left): Pressure and Streamline Plot for NACA 2414 at  $Re = 60k$ ,  $AoA = 12^\circ$

Figure 9 (right): Pressure and Streamline Plot for NACA 2414 at  $Re = 60k$ ,  $AoA = 14^\circ$

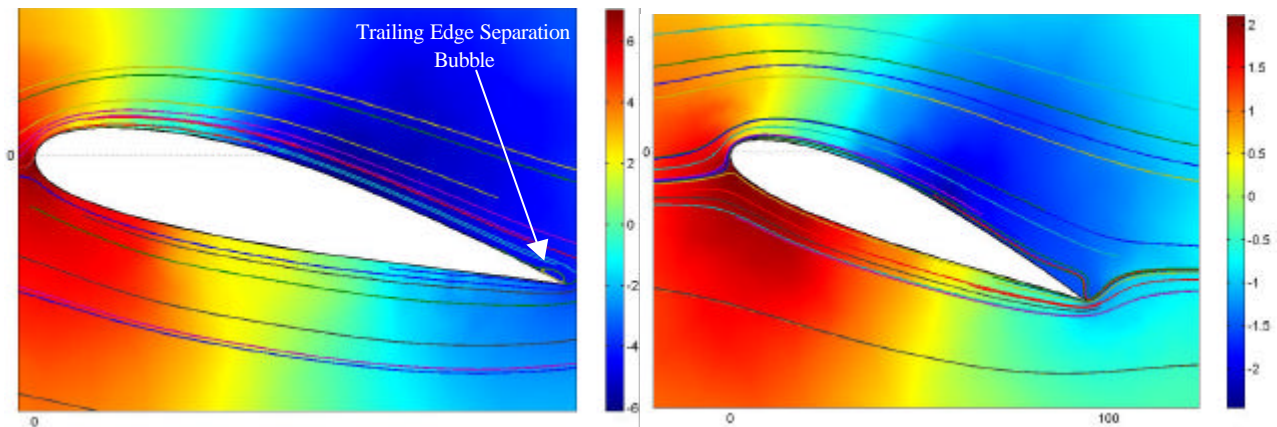


Figure 10 (left): Pressure and Streamline Plot for NACA 2415 at  $Re = 60k$ ,  $AoA = 12^\circ$

Figure 11 (right): Pressure and Streamline Plot for NACA 2415 at  $Re = 100k$ ,  $AoA = 18^\circ$

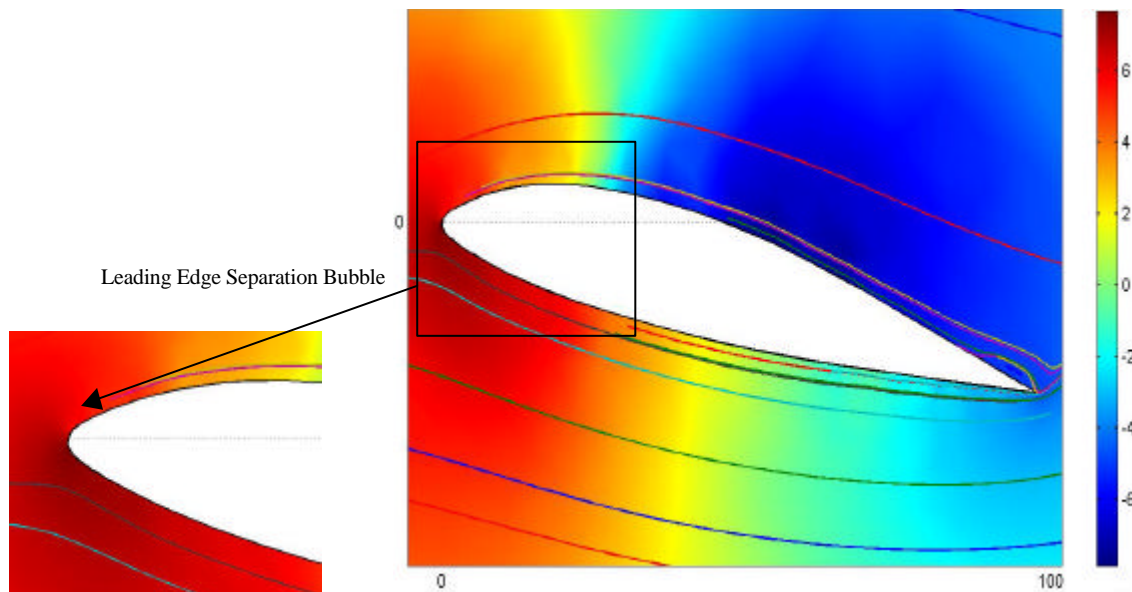


Figure 12: Pressure and Streamline Plot for MB253515 at  $Re = 60k$ ,  $AoA = 12^\circ$



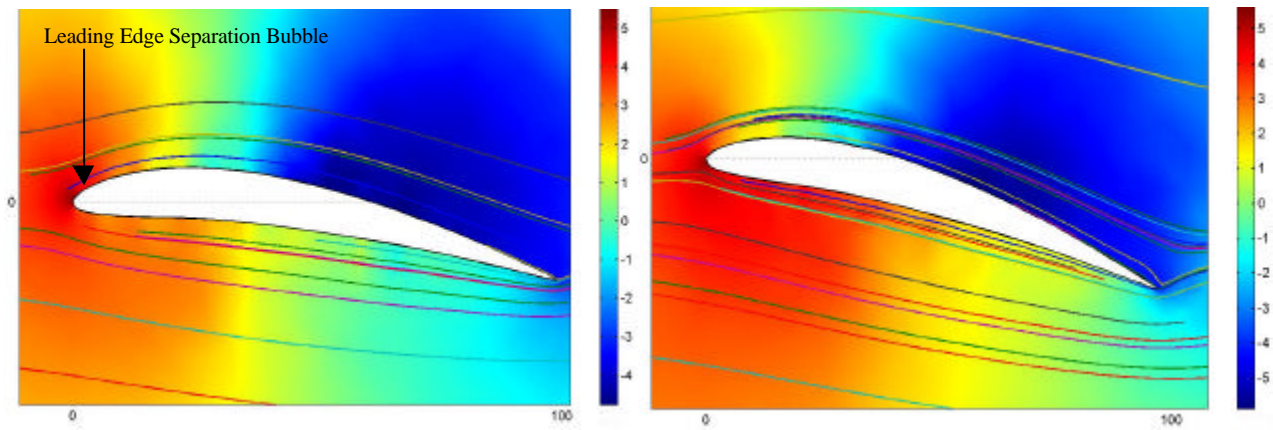


Figure 13 (left): Pressure and Streamline Plot for NACA 6409 at  $Re = 60k$ ,  $AoA = 8^\circ$   
 Figure 14 (right): Pressure and Streamline Plot for NACA 6409 at  $Re = 60k$ ,  $AoA = 14^\circ$

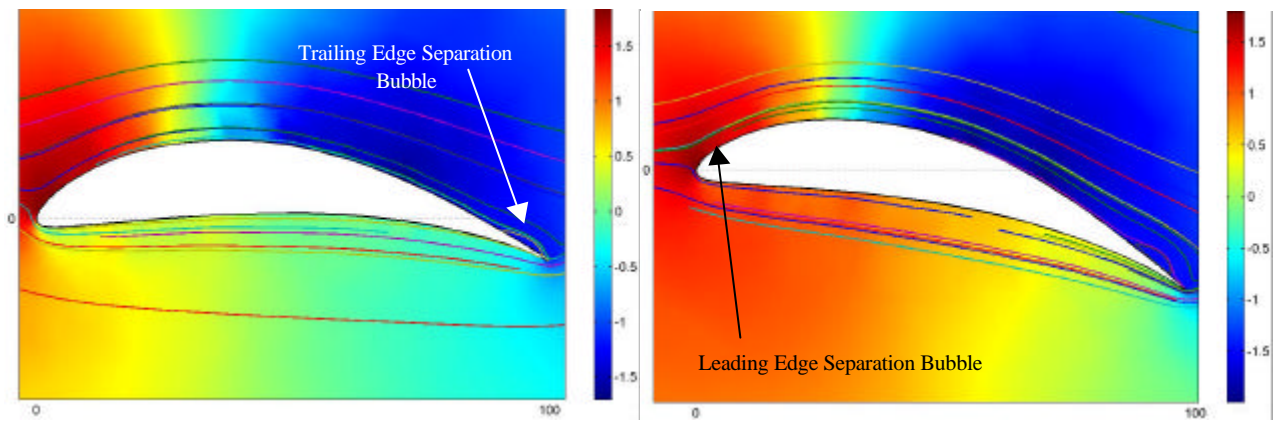


Figure 15 (left): Pressure and Streamline Plot for CH 10-48-13 at  $Re = 100k$ ,  $AoA = 4^\circ$   
 Figure 16 (right): Pressure and Streamline Plot for CH 10-48-13 at  $Re = 100k$ ,  $AoA = 12^\circ$

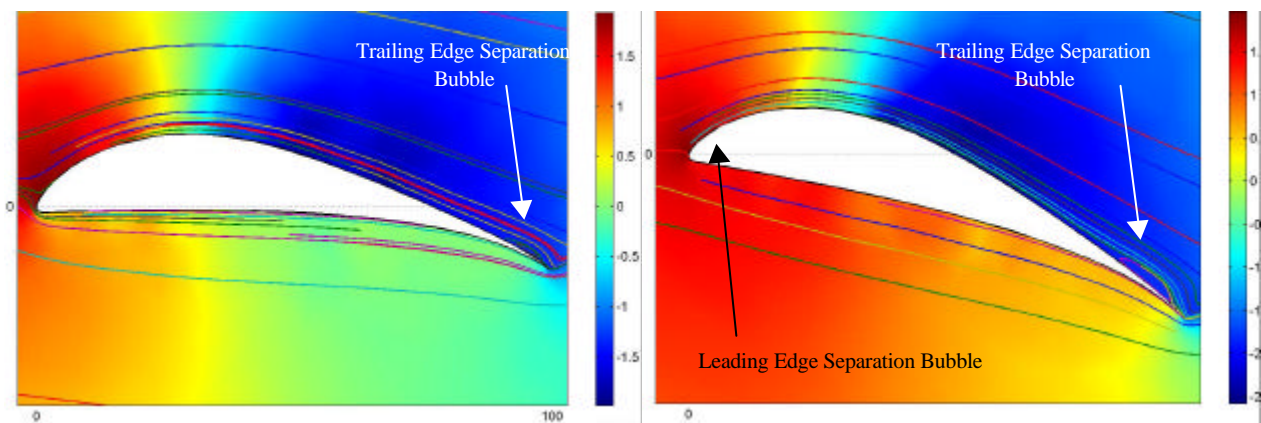


Figure 17 (left): Pressure and Streamline Plot for FX74-CL5-140 at  $Re = 100k$ ,  $AoA = 6^\circ$   
 Figure 18 (right): Pressure and Streamline Plot for FX74-CL5-140 at  $Re = 100k$ ,  $AoA = 16^\circ$

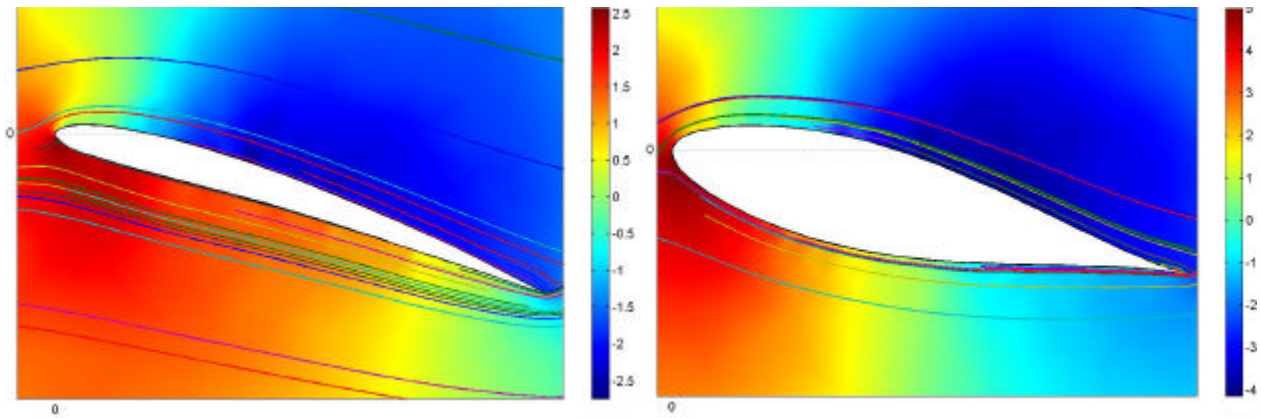


Figure 19 (left): Pressure and Streamline Plot for MA409 at  $Re = 40k$ ,  $AoA = 16^\circ$

Figure 20 (right): Pressure and Streamline Plot for NACA 633018 at  $Re = 40k$ ,  $AoA = 12^\circ$

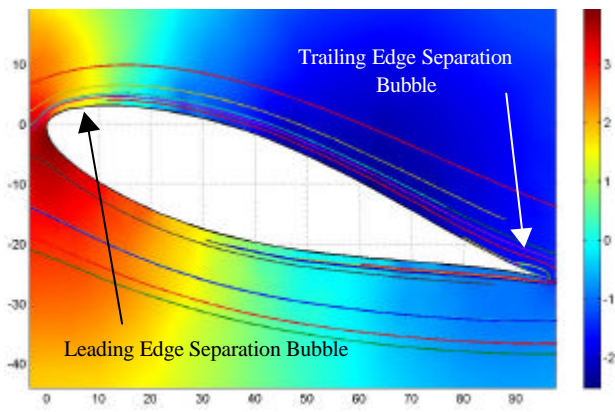
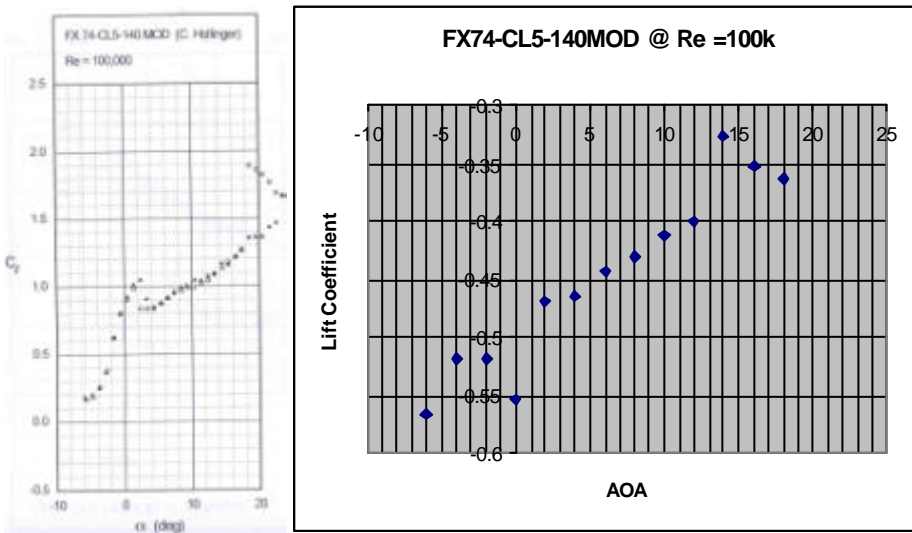
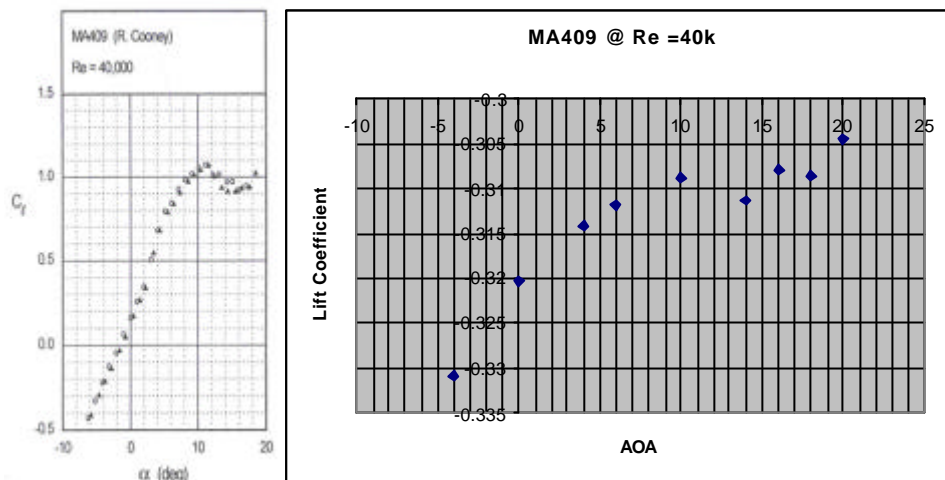


Figure 21: Pressure and Streamline Plot for NACA 633018 at  $Re = 40k$ ,  $AoA = 15^\circ$

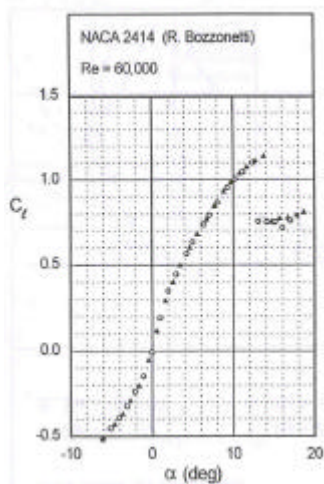


Graph 1: Comparison of  $C_L$  vs  $AoA$  Plots for Experimental and Femlab Simulation for FX74-CL5-140MOD Airfoil at  $Re = 100k$

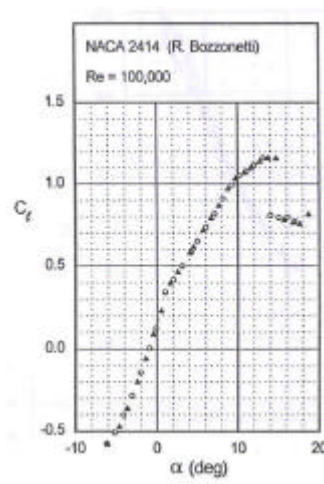
# CLASSIFICATION OF AIRFOILS BY ABNORMAL BEHAVIOR OF LIFT CURVES AT LOW REYNOLDS NUMBER



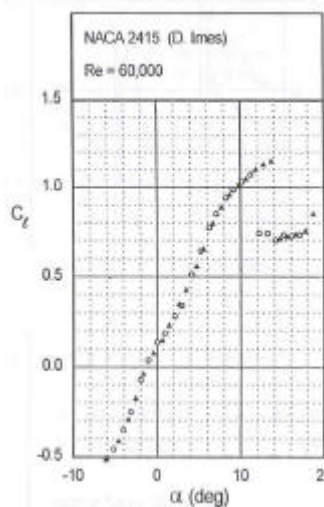
Graph 2: Comparison of  $C_L$  vs AoA Plots for Experimental and Femlab Simulation for MA409 Airfoil at  $Re = 40k$



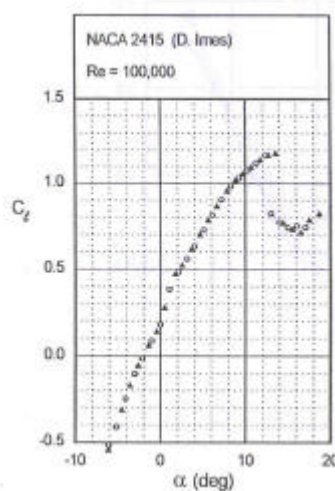
Graph 3: NACA 2414 Plot for  $Re = 60k$



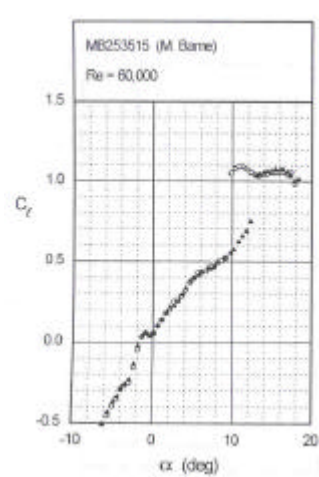
Graph 4: NACA 2414 Plot for  $Re = 100k$



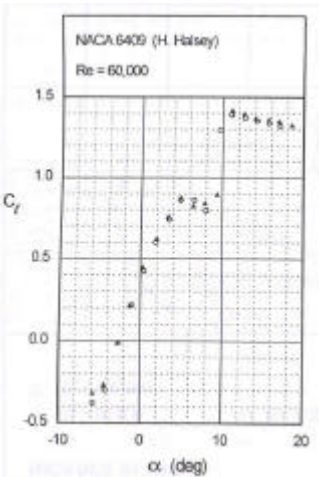
Graph 5: NACA 2415 Plot for  $Re = 60k$



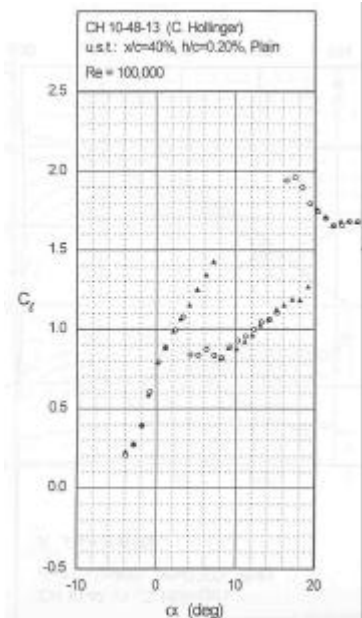
Graph 6: NACA 2415 Plot for  $Re = 100k$



Graph 7: MB253515 Plot for  $Re = 60k$



Graph 8: NACA 6409 Plot for  $Re = 60k$



Graph 9: CH 10-48-13 Plot for  $Re = 100k$